JOURNAL OF SOLID STATE CHEMISTRY 114, 42–51 (1995)

Structural, DSC, and IR Studies on a New Organic-Cation Cyclohexaphosphate: $[NH_3–(CH_2)_2–NH_2–(CH_2)_2–NH_3]_2P_6O_{18} \cdot 2H_2O$

A. Gharbi and A. Jouini[1]

Laboratoire de Chimie du Solide, Département de Chimie, Faculté des Sciences de Monastir, Université du centre, Monastir 5000, Tunisia

and

A. Durif

Laboratoire de cristallographie, associé à l'Université J. Fourier, CNRS, 166X, 38042, Grenoble Cédex 09, France

Received November 16, 1993; in revised form March 11, 1994; accepted March 17, 1994

Chemical preparation, calorimetric studies, crystal structure, and IR absorption spectra are given for a new organic cyclohexaphosphate. The aza-3 pentanediyl-1,5 dihydrate, $[NH_3–(CH_2)_2–NH_2–(CH_2)_2–NH_3]_2P_6O_{18} \cdot 2H_2O$ is triclinic $P\bar{1}$ with unit cell dimensions, $a = 8.709(2)$, $b = 9.729(2)$, $c = 9.145(2)$ Å, $\alpha = 99.11(2)°$, $\beta = 110.70(2)°$, $\gamma = 67.19(2)°$, and $Z = 1$, $V = 667.9(6)$ Å^3, $\rho_m = 1.72$ g · cm^{-3}, $\mu = 0.268$ mm^{-1}. The refinement of data, collected at room temperature, leads to a final $R = 0.035$ for 3844 independent reflections. The P_6O_{18} ring anion is centrosymmetric and significantly distorted with P–P–P angles varying from 93.6° to 134.8° as commonly observed for such rings with $\bar{1}$ internal symmetry. A three-dimensional network of strong hydrogen bonds interconnects the structural arrangement. Of the eight hydrogen atoms in the organic group, seven are connected to the external oxygen atoms of four phosphoric rings and form a complex anion of formula $[C_4N_3H_{16}(P_6O_{18})_4]^{-21}$; the remaining one establishes a hydrogen bond with a water molecule which links, with the help of its proper hydrogen atoms, successive complex anions. The hydrogen bonding geometries are discussed. © 1995 Academic Press, Inc.

INTRODUCTION

Schülke and Kayser (1) reported in 1985 an important improvement of the Griffith and Buxton process (2) for the preparation of $Li_6P_6O_{18}$. This good starting material opened the way for the characterization of cyclohexaphosphates. In spite of this work, the chemistry of this family of condensed phosphates was slow to develop and, even today, is poor if compared with the cyclotriphosphoric or cyclotetraphosphoric anions combined with organic or metallic cations. At present, three organic-cation cyclohexaphosphates, $[NH_3–(CH_2)_2–NH_3]_3P_6O_{18} \cdot 2H_2O$ (3), $[HO–NH_3]_6P_6O_{18} \cdot 4H_2O$ (4), and $[C_2H_5–NH_3]_6\ P_6O_{18} \cdot 4H_2O$ (5), and a series of isotypic organometallic cation compounds, $M[NH_3–(CH_2)_2–NH_3]_3P_6O_{18} \cdot 6H_2O$ (M = Cu, Co, Ni, Mg, Zn, Fe) (6) have been reported. They were characterized with small organic cations and prepared by the Boulle's process (7). The present work is devoted to determining the crystal structure and the physicochemical properties of a new organic cyclohexaphosphate obtained in a similar systematic study, but prepared with the help of the exchange ions resin and with a long chain organic cation, the aza-3 pentanediyl-1,5 diamine $NH_2–(CH_2)_2–NH–(CH_2)_2–NH_2$. We have previously described, with this organic molecule, two compounds, $C_4H_{15}N_3^{2+} \cdot HPO_4^{-2} \cdot 2H_2O$ (8) and $2C_4H_{15}N_3^{2+} \cdot P_4O_{12}^{-4} \cdot 4H_2O$ (9), in which the aza-3 is not protonated; in this work, we report what we believe is the first occurrence of a condensed phosphate molecule, in which all the electron-pair donor atoms are protonated. The chemical preparation, crystallographic features, detailed DSC, and IR analysis are reported.

II. CRYSTAL CHEMISTRY

1. Chemical Preparation

Chemical synthesis of the title compound was performed in two steps. A dilute aqueous solution of cyclohexaphosphoric acid was first prepared from 12 g of the starting material, $Li_6P_6O_{18}$ (1, 2), by using an ion exchange resin (Amberlite IR 120) (10). This solution was then slowly neutralized by adding 10 cm^3 of Aza-3 pentanediyl-1,5 diamine (density, 0.95). Schematically the reaction is

$$H_6P_6O_{18} + 2[NH_2–(CH_2)_2–NH–(CH_2)_2–NH_2] \rightarrow (H_2O) \rightarrow\rightarrow [NH_3–(CH_2)_2–NH_2–(CH_2)_2–NH_3]_2P_6O_{18} \cdot 2H_2O.$$

[1] To whom correspondence should be addressed.

0022-4596/95 $6.00

The resulting aqueous solution is slowly evaporated at room temperature. The crystallization produces, after 2 weeks, stout prismatic single crystals appropriate for structural investigation. The protonated aza-3 pentanediyl-1,5 diammonium cyclohexaphosphate dihydrate is stable under normal conditions of temperature and humidity.

2. *Crystal Data and Structure Determination*

The Weissenberg and oscillation photographs taken with Cu($K\alpha_1\alpha_2$) radiation show that the title compound crystallizes in the triclinic system. The unit cell dimensions, a = 8.716(2), b = 9.750(3), c = 9.148(3) Å, α = 99.07(4)°, β = 110.63(7)°, and γ = 67.63(4)°, have been measured and refined using a set of high-angle reflections collected with an Enraf–Nonius CAD4 diffractometer. The values obtained are used to index the low-scan-speed powder diffractogram reported in Table 1. The structural determination shows that the proper space group is the centrosymmetric $P\bar{1}$. The average density value, ρ_m = 1.72 g · cm^{-3}, measured at room temperature using bromobenzene as the pycnometric liquid, is in agreement with the calculated ρ_x = 1.752 g · cm^{-3}. The cell contains one formula unit of the title compound. The parameters used for X-ray diffraction data collection, as well as the strategy used for the crystal structure determination and its final results, are reported in Table 2. The final atomic coordinates and their equivalent temperature factors, isotropic for H atoms, are given in Table 3. The values of the thermal anisotropic displacement parameters for nonhydrogen atoms and the list of observed and calculated structure factors are available on request.

3. *Thermal Behavior*

TGA and DSC studies are carried out with a Setaram TG70 and a DSC92. TGA experiments are done with 140-mg samples in an open silica crucible and heated from 300 to 723 K at various rates in an air atmosphere. DSC anal-

TABLE 1
Indexed Powder Diagram of $[NH_3–(CH_2)_2–NH_2–(CH_2)_2–NH_3]_2P_6O_{18} \cdot 2H_2O$

h k l	$d_{obs.}$	$d_{calc.}$	$I_{obs.}$	h k l	$d_{obs.}$	$d_{calc.}$	$I_{obs.}$
0 1 0	8.96	8.97	18	1 $\bar{2}$ 1		3.010	
0 0 1	8.55	8.55	100	1 1 $\bar{3}$	3.007	3.005	13
1 0 0	7.60	7.60	10	$\bar{1}$ 0 3		3.005	
$\bar{1}$ 0 1	6.88	6.88	55	0 3 0	2.986	2.989	9
0 1 1	6.11	6.11	14	2 3 $\bar{2}$	2.778	2.781	24
$\bar{1}$ 1 0	4.98	4.98	6	0 $\bar{1}$ 3	2.733	2.736	8
1 0 1		4.95		3 2 $\bar{2}$		2.721	
$\bar{1}$ 1 1	4.72	4.73	18	2 $\bar{1}$ 1	2.718	2.717	15
1 2 0	4.66	4.66	8	1 2 $\bar{3}$		2.716	
1 2 $\bar{1}$	4.53	4.54	11	1 $\bar{2}$ 2		2.500	
0 2 0	4.48	4.48	21	1 $\bar{3}$ 0	2.491	2.493	8
$\bar{1}$ 0 2		4.38		$\bar{2}$ 2 0		2.491	
1 1 $\bar{2}$	4.37	4.35	53	0 $\bar{3}$ 2	2.471	2.478	14
2 1 $\bar{1}$		4.31		2 0 $\bar{2}$		2.474	
0 0 2	4.28	4.28	30	2 2 2		2.400	
2 $\bar{1}$ 0	4.06	4.06	27	$\bar{1}$ 1 3	2.398	2.399	20
0 $\bar{2}$ 1		4.01		1 4 0		2.396	
$\bar{2}$ 0 1	3.980	3.980	25	0 2 $\bar{3}$	2.377	2.379	7
1 $\bar{1}$ 1		3.978		2 4 $\bar{2}$	2.268	2.270	8
2 0 0	3.792	3.802	71	2 $\bar{1}$ 2		2.261	
$\bar{2}$ 2 $\bar{1}$		3.795		$\bar{1}$ 3 2		2.238	
$\bar{1}$ 1 2	3.610	3.615	30	$\bar{3}$ 1 0	2.235	2.237	5
2 2 0		3.608		1 4 1		2.234	
$\bar{2}$ 0 2	3.437	3.442	12	$\bar{2}$ 0 4	2.186	2.187	48
$\bar{1}$ 2 0	3.366	3.368	18	3 4 $\bar{1}$		2.183	
1 0 2	3.297	3.302	22	2 4 1		2.132	
$\bar{1}$ 2 1	3.271	3.275	31	1 2 $\bar{4}$	2.130	2.131	7
1 1 2	3.241	3.246	63	4 1 $\bar{1}$		2.129	
$\bar{2}$ 1 1	3.197	3.206	24	1 4 2		1.985	
1 3 0		3.200		$\bar{3}$ 2 1	1.984	1.984	10
1 3 $\bar{1}$	3.166	3.170	20	3 4 $\bar{3}$		1.981	
2 0 1	3.118	3.122	31	1 5 $\bar{1}$		1.903	
$\bar{2}$ 1 0		3.120		4 0 0	1.900	1.901	5
0 2 2	3.054	3.057	6	4 4 $\bar{2}$		1.897	

TABLE 2

Main Crystallographic Features, X-ray Diffraction Data Collection Parameters, Strategy Used for the Crystal Structure Determination of $[NH_3–(CH_2)_2–NH_2–(CH_2)_2–NH_3]_2P_6O_{18} \cdot 2H_2O$ and Its Final Results

Crystal data	
Formula: $(C_4H_{16}N_3)_2P_6O_{18} \cdot 2H_2O$	$F_w = 722.243$
Crystal system: triclinic	Space group: $P\bar{1}$
$a = 8.709(2)$, $b = 9.729(2)$	$V = 667.9(6)$ Å^3
$c = 9.145(2)$ Å, $\alpha = 99.11(2)°$	
$\beta = 110.70(2)°$, $\gamma = 67.19(2)°$	$Z = 1$
$\rho_{cal.}$, $\rho_{mes.} = 1.795$, 1.72 g · cm^{-3}	$F(000) = 376$
Linear absorption factor:	$\mu(AgK_\alpha) = 0.268$ mm^{-1}
Morphology:	elongated triclinic prism
Crystal size:	0.18 × 0.26 × 0.28 mm
Intensity measurements	
Temperature: 298K	Wavelength: AgK_α (0.5608 Å)
Diffractometer: Nonius CAD4	Scan mode: ω
Monochromator: graphite plate	Scan width: 1.20°
Variable scan speed	T_{max} per scan: 60 sec
Theta range:	2–30°
Background measuring time:	$T_{max}/2$
Measurement area: $\pm h$, $\pm k$, l	$h_{max} = 15$, $k_{max} = 17$, $l_{max} = 16$
Number of scanned reflections:	8303
Number of nonzero reflections:	4393
Number of collected unique reflections:	4239 ($R_{int.} = 0.015$)
Reference reflections: $\bar{1}\ 5\ \bar{2}$, $1\ \bar{5}\ 2$,	every 2 hr, no variation
Structure determination	
Lorentz and polarization corrections	No absorption correction
Program used: SDP [11]	Computer used: Micro-Vax II
Determination:	Direct methods with MULTAN [12]
Unique reflections included:	3844 with $I > 3\sigma(I)$
Weighting scheme: unitary	Refined parameters: 253
Secondary extinction coefficient:	not applied
Unweighted agreement factor R:	0.035
Weighted agreement factor R_w:	0.038
ESD: 0.655	Largest shift/error = 0.41
Maximum residual density:	0.41 e · Å^{-3}

ysis is carried out using weighted 13-mg samples sealed in an aluminum DSC crucible; an empty aluminum crucible is used as reference. Samples are heated from 293 to 543 K in an air atmosphere at different heating rates, varying from 3 to 15 K · min^{-1}.

From the TGA weight loss curve (Fig. 1), we deduce two molecules of water per formula unit. The dehydration occurs in one large step in the temperature range 358–446 K with a maximum at 408 K. The compound decomposes with maximum elimination of NH_3 at 603 K.

Figure 2a, showing the DSC thermogram of $[NH_3–(CH_2)_2–NH_2–(CH_2)_2–NH_3]_2P_6O_{18} \cdot 2H_2O$ in the heating run, reveals three pronounced endothermic effects. The first two peaks correspond to the loss of the two water molecules between 360 and 407 K with peak temperature maxima at 371 and 396 K; the third one is due to the melting of the sample corresponding to the irreversible phase change from crystalline to amorphous at 415 K. The differential calorimetric study gives an overall ΔH for the dehydration of the compound of 98 + 253.9 = 351.9 kJ · mol^{-1}; the enthalpy change for the melting of this compound is 90.14 KJ · mol^{-1}. The shapes of the endotherms exhibit a long induction period followed by a short reaction period, and these are obviously distinct.

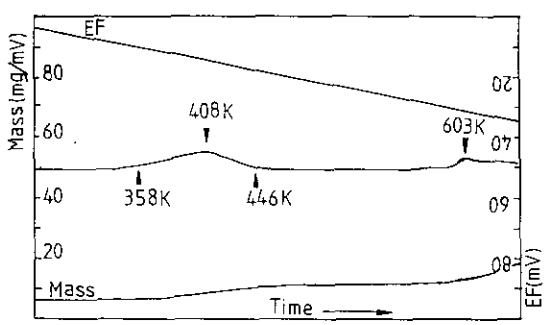

FIG. 1. TGA of $[NH_3–(CH_2)_2–NH_2–(CH_2)_2–NH_3]_2P_6O_{18} \cdot 2H_2O$.

TABLE 3
Final Atomic Coordinates and B_{eq}, (b_{iso} for H-Atoms) of $[NH_3–(CH_2)_2–NH_2–(CH_2)_2–NH_3]_2P_6O_{18} \cdot 2H_2O$

Atoms	$x(\sigma)$	$y(\sigma)$	$z(\sigma)$	B_{eq} (Å^2)
P(1)	0.21891(6)	0.07323(5)	0.86124(6)	1.288(8)
P(2)	0.36584(6)	−0.24689(5)	0.91768(5)	1.236(8)
P(3)	0.34527(5)	0.28555(5)	0.78375(5)	1.112(7)
O(E11)	0.1843(2)	0.1633(2)	1.0004(2)	2.46(3)
O(E12)	0.0698(2)	0.0512(2)	0.7310(2)	2.35(3)
O(L12)	0.3681(2)	−0.0843(2)	0.9188(2)	2.40(3)
O(L13)	0.3296(2)	0.1289(1)	0.7933(2)	1.59(2)
O(E21)	0.2290(2)	−0.2408(2)	0.9815(2)	2.17(3)
O(E22)	0.3698(2)	−0.3236(2)	0.7653	2.55(4)
O(L23)	0.4408(2)	0.3238(1)	0.9623(2)	1.46(2)
O(E31)	0.1679(2)	0.4014(2)	0.7368(2)	1.97(3)
O(E32)	0.4629(2)	0.2548(2)	0.6894(2)	1.71(3)
O(W)	0.2398(3)	0.7571(3)	0.4636(2)	3.66(5)
N(1)	0.7746(2)	0.0097(2)	0.7494(2)	1.85(3)
N(2)	0.9230(2)	0.6646(2)	0.7518(2)	1.50(3)
N(3)	0.6781(2)	0.4319(2)	0.7788(2)	1.89(3)
C(1)	0.7535(3)	0.9078(2)	0.6107(2)	1.80(4)
C(2)	0.0906(2)	0.2368(2)	0.3662(2)	1.63(3)
C(3)	0.7785(3)	0.6051(2)	0.7040(3)	2.11(4)
C(4)	0.1843(2)	0.5021(2)	0.1739(2)	1.79(3)
H(1W)	0.274(5)	0.747(4)	0.562(4)	3.0(9)*
H(2W)	0.138(5)	0.809(4)	0.432(4)	4.0(9)*
H(1N1)	0.683(5)	0.095(4)	0.734(4)	2.8(9)*
H(2N1)	0.789(4)	0.970(4)	0.832(4)	2.4(8)*
H(3N1)	0.135(4)	0.968(4)	0.232(4)	2.6(9)*
H(1N2)	0.929(4)	0.715(4)	0.837(4)	2.2(8)*
H(2N2)	0.029(4)	0.590(4)	0.765(4)	2.6(9)*
H(1N3)	0.686(4)	0.378(4)	0.695(4)	2.5(9)*
H(2N3)	0.304(4)	0.627(4)	0.140(4)	2.8(9)*
H(3N3)	0.442(5)	0.497(4)	0.233(4)	3.0(9)*
H(1C1)	0.246(5)	0.055(4)	0.490(4)	2.8(9)*
H(2C1)	0.650(5)	0.883(4)	0.574(4)	2.8(9)*
H(1C2)	0.024(4)	0.780(4)	0.667(4)	2.3(8)*
H(2C2)	0.099(4)	0.287(4)	0.465(4)	2.1(8)*
H(1C3)	0.663(5)	0.686(4)	0.698(4)	2.9(9)*
H(2C3)	0.764(4)	0.561(4)	0.600(4)	2.4(9)*
H(1C4)	0.072(4)	0.589(4)	0.165(4)	2.1(8)*
H(2C4)	0.176(4)	0.462(4)	0.072(4)	2.5(9)*

Note. Starred atoms were determined isotropically. ESDs are given in parentheses. $B_{eq} = 4/3 \Sigma_i \Sigma_j \mathbf{a}_i \cdot \mathbf{b}_j \cdot \beta_{ij}$.

An additional thermal treatment in the carbolite furnace, with a scanning speed of 5 K · min^{-1} from room temperature to 407 K (below the melting point), followed by IR spectroscopic and RX powder diffraction tests on the remaining compound reveals the presence of the infrared absorption bands characteristic of the cyclic anion $P_6O_{18}^{-6}$ and a well-crystallized anhydrous compound. Heated at 420 K in this furnace, the anhydrous compound melts and does not crystallize when cooled at room temperature but becomes a supercooled liquid. Hence, the crystallization has been supressed entirely, and hysteresis is so great that crystallization has not occurred. In this case, the liquid is very viscous even above the melting point, and crystallization is very slow, even at slow cooling rates. Apparently, the compound is polymerized and an amorphous phase, as confirmed by RX powder diffraction, is formed.

Differential calorimetric study, in which the anhydrous compound was heated at a rate of 10 K · min^{-1}, reveals a broad anomaly in the baseline of the DSC curve preceding the irreversible phase change due to the glass transition at 437 K, as shown in Fig. 2b (not observed with the third peak of Fig. 2a). The maximum of the endothermic peak corresponding to this phase change is shifted to 443 K; the higher the heating rate, the higher the maximum temperature of the endothermic peak (13, 14). The heat capacity measurement on the DSC cell, gives a value of 0.197 J · g^{-1} · °C^{-1}. However, the stability of the compound is not very high since the aza-3 pentanediyl-1,5 diammonium decomposes between 480 and 500 K with maximum elimination of NH_3 at 494 K. Within this temperature range, a rather bad smell escapes from the resulting black compound. It is to be noted that in the presence of the amorphous phase, where phosphorous is abundant, the title compound at 459 K already forms homogeneous melts with a complex anionic composition. However, recent investigation of thermal behavior shows that the ultimate decomposition of the mineral cyclohexaphosphates, $K_6P_6O_{18} \cdot 3H_2O$ (15) and $Cr_2P_6O_{18} \cdot 21H_2O$ (16) leads to the formation of linear polyphosphate anions.

III. STRUCTURE DESCRIPTION

Figures 3 and 4 report projections of the atomic arrangement along the [001] and [101] directions. Figure 3 shows the facial P_6O_{18} ring configuration, whereas Fig. 4 exhibits the sideface of the isolated cyclic anions in the cell. For clarity, the aza-3 pentanediyl-1,5 diammonium and the water molecules are illustrated without their hydrogen atoms.

1. The $P_6O_{18}^{-6}$ Ring Anion

The main geometrical features of this ring are reported in Table 4. Like the majority of the 30 presently known P_6O_{18} configurations, all of which were observed in accurate structure determinations of cyclohexaphosphates (6), the P_6O_{18} ring of the title compound has a $\bar{1}$ internal symmetry. It develops around the inversion center located at (0, 0, ½) and so is built up by only three independent PO_4 tetrahedra. This ring is significantly distorted; the P–P–P angles vary between 93.6° and 134.8°. These angles, which average 111.2°, show very large deviations from the ideal value of 120° compared to the other types of well-represented phosphoric rings such as cyclotri- and cyclotetraphosphates, in which the P–P–P angles never

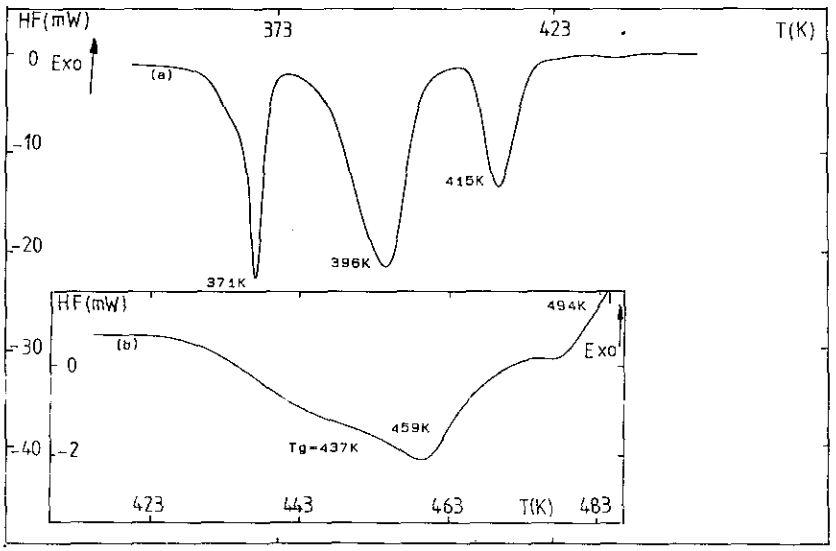

FIG. 2. (a) DSC curve for $[NH_3-(CH_2)_2-NH_2-(CH_2)_2-NH_3]_2P_6O_{18} \cdot 2H_2O$. The first two peaks correspond to the dehydration, the third one to the irreversible phase change from crystalline to amorphous. (b) DSC curve for the anhydrous $[NH_3-(CH_2)_2-NH_2-(CH_2)_2-NH_3]_2P_6O_{18}$ compound showing the T_g preceding the phase change and the elimination of NH_3 groups.

depart significantly from their ideal values of 60 ± 2° for cyclotriphosphates and 90 ± 4° for cyclotetraphosphates. Nevertheless this distortion is comparatively less important than that observed in $Cs_6P_6O_{18} \cdot 6H_2O$ which shows the greatest distortion for the same angles spreading between 93.2 and 145.5° (6). The great flexibility of the

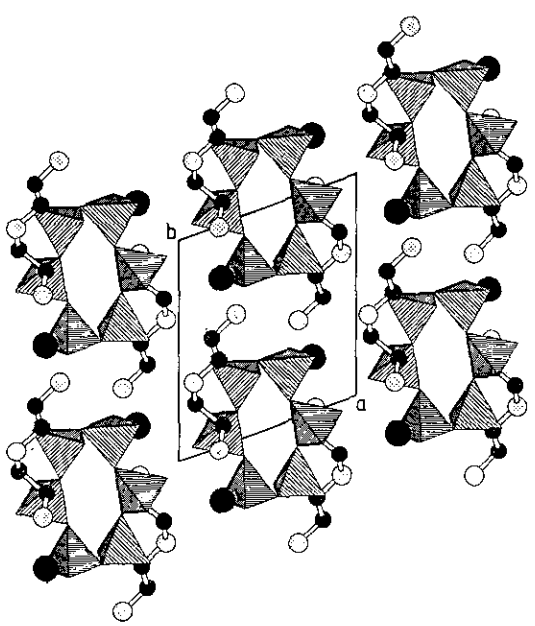

FIG. 3. Projection along the [001] direction of the atomic arrangement showing the facial P_6O_{18} ring configuration given with a polyhedral representation. Black circles represent water molecules. Larger dotted circles are nitrogen; smaller dotted circles carbon atoms. Hydrogen atoms have been omitted.

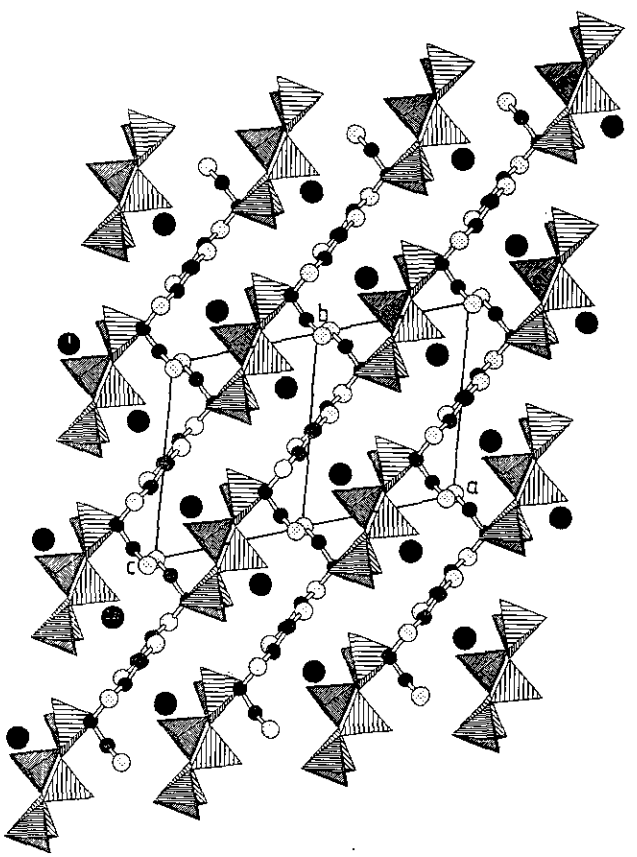

FIG. 4. Projection along the [101] direction of the atomic arrangement showing the side face P_6O_{18} ring given with a polyhedral representation. The larger black circles represent the water–oxygen atoms, and the smaller, dotted circles and the cross-hatched circles are nitrogen and carbon atoms, respectively.

TABLE 4
Main Interatomic Distances (Å) and Bond Angles (°) in $[NH_3-(CH_2)_2-NH_2-(CH_2)_2-NH_3]_2P_6O_{18} \cdot 2H_2O$

The Phosphoric Group

$P(1)O_4$ tetrahedron

P(1)	O(E11)	O(E12)	O(L12)	O(L13)
O(E11)	1.482(2)	119.0(1)	108.2(1)	111.4(1)
O(E12)	2.554(2)	1.483(2)	109.9(1)	109.3(1)
O(L12)	2.496(2)	2.523(2)	1.598(1)	96.7(1)
O(L13)	2.543(3)	2.513(3)	2.387(2)	1.596(2)

$P(2)O_4$ tetrahedron

P(2)	O(E21)	O(E22)	O(L12)	O(L23)
O(E21)	1.480(2)	119.1(1)	109.9(1)	111.0(1)
O(E22)	2.551(3)	1.479(2)	110.5(1)	105.4(1)
O(L12)	2.515(3)	2.524(2)	1.591(2)	99.1(1)
O(L23)	2.547(2)	2.457(2)	2.434(2)	1.608(1)

$P(3)O_4$ tetrahedron

P(3)	*O(E31)*	*O(E32)*	*O(L13)*	*O(L23)*
O(E31)	1.478(1)	120.4(1)	109.5(1)	106.5(1)
O(E32)	2.567(2)	1.480(2)	105.3(1)	110.3(1)
O(L13)	2.516(2)	2.451(3)	1.603(2)	103.7(1)
O(L23)	2.475(2)	2.536(2)	2.526(2)	1.609(1)

P(1)–P(2)	2.932(1)	P(2)–P(1)–P(3)	134.78(2)
P(1)–P(3)	2.963(1)	P(1)–P(2)–P(3)	105.22(2)
P(2)–P(3)	2.947(1)	P(1)–P(3)–P(2)	93.59(1)
		P(1)–O(L12)–P(2) 133.7(1)	
		P(1)–O(L13)–P(3) 135.7(1)	
		P(2)–O(L23)–P(3) 132.7(1)	

Note. ESDs are given in parentheses.

P_6O_{18} ring can probably explain the strong stability of cyclohexaphosphates. Examination of the main geometrical features (cf. Table 4) of the three independent PO_4 tetrahedra shows clearly that, in spite of the P–P–P angles deformation, they are in accordance with all that has been previously observed for PO_4 tetrahedra involved in condensed phosphate anions. Indeed, three different types of O–P–O angles coexist in PO_4 tetrahedra. The O(L)–P–O(L) corresponding to the largest P–O bonds are always close to 100°. The O(L)–P–O(E) angles have values expected for a regular tetrahedron, while the O(E)–P–O(E) corresponding to the shortest P–O distances always have large values close to 120°, probably induced by the mutual repulsion of the nonbridging oxygen atoms. Nevertheless, the calculated average values of the distortion indices (17) corresponding to the different angles and distances in the independent PO_4 tetrahedra, DI(PO) = 0.0218, DI(OPO) = 0.0268, and DI(OO) = 0.0036 show a pronounced distortion of the P–O distances if compared to O–O distances. The PO_4 tetrahedron is then described by a regular oxygen atom arrangement with the phosphorous atom shifted from the center of gravity. The PO_4 tetrahedron will have $3m$ internal symmetry instead of $\bar{4}$ $3m$ ideal symmetry.

2. *The Aza-3 Pentanediyl-1,5 Diammonium Groups and Hydrogen Bonds*

The only crystallographically independent trication $NH_3^+-(CH_2)_2-NH_2^+-(CH_2)_2-NH_3^+$, present in this atomic arrangement has no internal symmetry. All distances and angles relating to the conformation of this group are reported in Table 5. N–C and C–C distances and N–C–C and C–N–C angles are similar; for instance, they spread within the respective ranges 1.477 to 1.515 Å and 108.7° to 114.0°. The geometrical features measured in aza-3 pentanediyl-1,5 diammonium are quite similar to the one previously observed for this group involved in phosphate anions such as HPO_4^{-2} (8) and $P_4O_{12}^{-4}$ (9); the only exception is that all the electron-pair donor atoms are protonated in this case. Among the eight hydrogen atoms of this group only, one, H(1N3), establishes a hydrogen bond with a water molecule; the remaining ones are connected to the external oxygen atoms of four phosphoric rings to form a complex anion of formula $[C_4N_3H_{16}(P_6O_{18})_4]^{-21}$, as

TABLE 5
Main Interatomic Distances (Å) and Bond Angles (°) in the Aza-3 Pentanediyl-1,5 Diammonium

$NH_3-(CH_2)_2-NH_2-(CH_2)_2-NH_3$ Group

N(1)–H(1N1)	0.89(3)	H(1N1)–N(1)–H(2N1)	110(4)
N(1)–H(2N1)	*0.85(4)*	*H(1N1)–N(1)–H(3N1)*	*107(4)*
N(1)–H(3N1)	0.85(4)	H(2N1)–N(1)–H(3N1)	106(4)
N(2)–H(1N2)	0.85(3)		
N(2)–H(2N2)	0.91(3)	H(1N2)–N(2)–H(2N2)	108(3)
N(3)–H(1N3)	0.86(4)	H(1N3)–N(3)–H(2N3)	110(4)
N(3)–H(2N3)	0.94(4)	H(1N3)–N(3)–H(3N3)	113(3)
N(3)–H(3N3)	0.99(3)	H(2N3)–N(3)–H(3N3)	101(4)
C(1)–H(1C1)	1.04(5)		
C(1)–H(2C1)	0.96(4)	H(1C1)–C(1)–H(2C1)	103(3)
C(2)–H(1C2)	1.01(4)		
C(2)–H(2C2)	0.95(3)	H(1C2)–C(2)–H(2C2)	105(3)
C(3)–H(1C3)	1.00(3)		
C(3)–H(2C3)	0.97(3)	H(1C3)–C(3)–H(2C3)	105(3)
C(4)–H(1C4)	1.00(3)		
C(4)–H(2C4)	0.94(3)	H(1C4)–C(4)–H(2C4)	106(3)
N(1)–C(1)	1.486(3)	N(1)–C(1)–C(2)	111.7(1)
C(1)–C(2)	1.513(2)	C(1)–C(2)–N(2)	113.9(2)
C(2)–N(2)	1.501(4)	C(2)–N(2)–C(3)	114.0(1)
N(2)–C(3)	1.478(3)	N(2)–C(3)–C(4)	108.7(2)
C(3)–C(4)	1.515(3)	C(3)–C(4)–N(3)	110.1(2)
C(4)–N(3)	1.477(3)		

Note. ESDs are given in parentheses.

shown in Fig. 5. The two hydrogen atoms from the water molecule act as a link between successive complex anions. A three-dimensional network of strong hydrogen bonds interconnects the structural arrangement. The structure contains short, strong N–H ··· O–P and O–H ··· O–P hydrogen bonds. The range of N(O) ··· O distances is quite narrow, 2.762–2.896 Å, except for the very short 2.649 Å bond, N(2)–H2 ··· O(E13). There are, then, two types of N(O)–H donors, viz., weaker ammonium $-NH_3$ and O–H donors as well as stronger aza-3 >N–H donors. The main geometric features of the hydrogen bonds are described in Table 6. As is usual in compounds involving phosphoric anions, the bonding O(L) atoms do not take part in such a network. This structure includes equal numbers of potential hydrogen bond donors and acceptors, eight N–H and two O–H donors and ten O or OH acceptors. All of the N–H groups do function as donors, but both O–H groups are donors and acceptors. Among the acceptor atoms, three external oxygen atoms O(E11), O(E21), and O(E22) are double acceptors; the others are single acceptors.

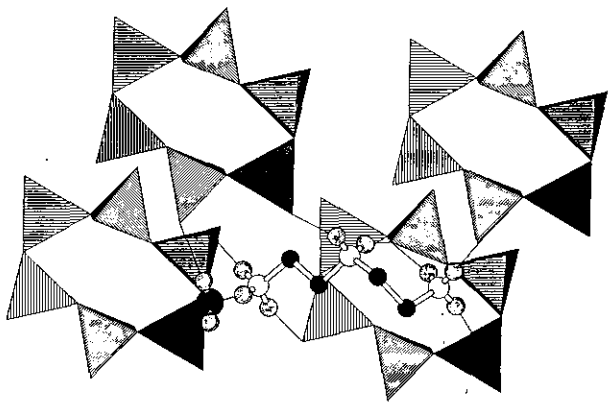

FIG. 5. Hydrogen-bond scheme connecting phosphoric rings in $[NH_3–(CH_2)_2–NH_2–(CH_2)_2–NH_3]_2P_6O_{18} \cdot 2H_2O$.

IV. IR INVESTIGATION

Infrared spectra were recorded by using a "Perkin–Elmer 983" spectrometer. Samples were dispersed in KBr and scanning was performed in the 4000–200 cm^{-1} spectral domain with a resolution of about 3 cm^{-1}.

One of the basic difficulties encountered in trying to interpret the vibrational spectrum (Fig. 6) of the title compound is the lack of experimentally determined fundamental vibrational frequencies of cyclohexaphosphates. However, some theoretical studies of silicon–oxygen rings of symmetry D_{nh} (18), in particular, a study of the symmetrical group Si_6O_{18} involved in the beryl, $Al_2Be_3Si_6O_{18}$ (19), are needed for an objective assignment. A detailed vibrational analysis of IR spectra of cyclohexaphosphates has not been done as yet. However, the IR spectra of cyclophosphates are always recognizably different, although the general regions of absorption for the cyclic anions are not greatly different (20–24), for that the same atomic group motions are involved. Theoretical group analysis applied to an isolated P_6O_{18} ring with an ideal symmetry of D_{6h} leads to the internal modes

$$\Gamma_{int} = 4A_{1g} + 2A_{2g} + 2B_{1g} + 3B_{2g} + 4E_{1g} + 7E_{2g} + A_{1u} + 3A_{2u} + 4B_{1u} + 3B_{2u} + 6E_{1u} + 5E_{2u},$$

where only A_{2u} and E_{1u} species are active in IR and A_{1g}; E_{1g} and E_{2g} species are active in Raman. The 66 internal modes are separated in 24 stretching modes,

$$\Gamma_{stretch} = A_{2u} + B_{2g} + E_{1g} + E_{2u} + 2B_{1u} + 3E_{1u} + 3E_{2g} + A_{2g} + B_{2u},$$

TABLE 6
Hydrogen-bond Scheme in $[NH_3–(CH_2)_2–NH_2–(CH_2)_2–NH_3]_2P_6O_{18} \cdot 2H_2O$

	N(O)–H	H ··· O	N(O) ··· O	N(O)–H ··· O
N(1)–H(1N1) ··· O(E23)	0.89(3)	1.90(3)	2.780(2)	170(4)
N(1)–H(2N1) ··· O(E11)	0.85(4)	2.05(4)	2.896(3)	168(4)
N(1)–H(3N1) ··· O(E21)	0.58(4)	2.01(5)	2.818(3)	158(4)
N(2)–H(1N2) ··· O(E11)	0.85(3)	2.04(4)	2.812(2)	151(3)
N(2)–H(2N2) ··· O(E13)	0.91(3)	1.80(3)	2.649(2)	153(4)
N(3)–H(1N3) ··· O(W)	0.86(3)	1.91(4)	2.762(3)	167(4)
N(3)–H(2N3) ··· O(E12)	0.94(3)	1.86(4)	2.794(4)	170(4)
N(3)–H(3N3) ··· O(E22)	0.99(3)	1.84(4)	2.797(2)	163(4)
O(W)–H(1W) ··· O(E22)	0.85(4)	1.87(4)	2.705(3)	167(4)
O(W)–H(2W) ··· O(E21)	0.80(3)	2.05(3)	2.776(2)	151(5)
H(1W)–O(W)–H(2W)	111(4)			

Note. ESDs are given in parentheses.

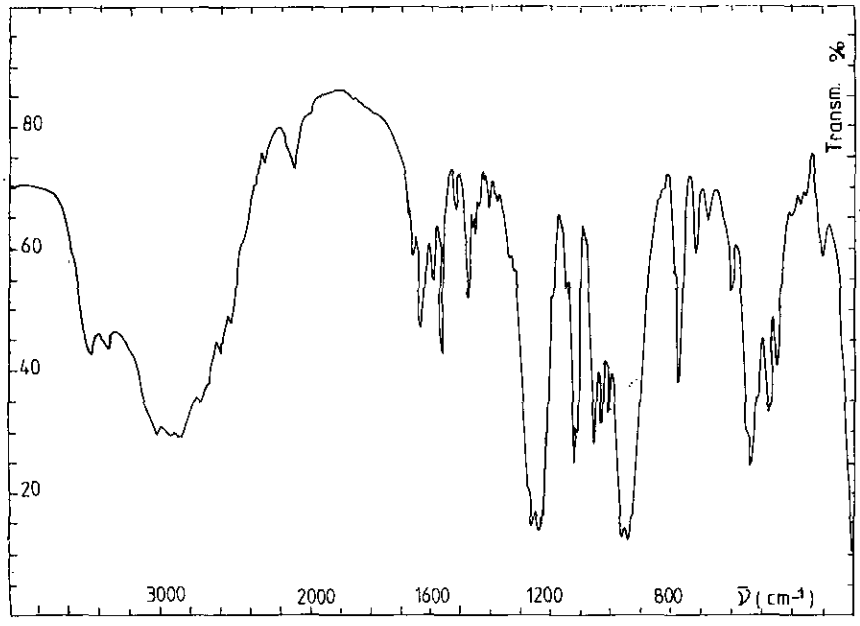

FIG. 6. IR spectrum of polycrystalline $[NH_3–(CH_2)_2–NH_2–(CH_2)_2–NH_3]_2P_6O_{18} \cdot 2H_2O$.

and in 42 bending modes,

$$\Gamma_{bend} = 2A_{2u} + 2B_{2g} + 3E_{1g} + 4E_{2u} + 2B_{1u} + 3E_{1u} + 4E_{2g} + A_{2g} + 2A_{1g} + 2B_{1g} + 2B_{2u} + A_{1u}.$$

We note that theoretically the IR and Raman active modes are distinguishable and there is one IR active mode, A_{2u} or E_{1u} in each of the four stretching vibration domains (Table 7). In the lattice, the only P_6O_{18} ring has a C_i site of symmetry lower than the ideal D_{6h} symmetry. This may lead to the activation of inactive modes along with shifting and splitting of the internal modes. At the C_i site, the 66 normal modes predicted by the theoretical group analysis for P_6O_{18} ring are distributed as $\Gamma_{int} = 33A_u + 33_{Ag}$ and only the A_u mode is IR active. According to the previous studies of cyclohexasilicates (19, 25, 26) and based on the only observed frequencies in cyclohexaphosphate $Cr_2P_6O_{18} \cdot 21H_2O$ (14), the stretching P–O modes of P_6O_{18} ring are observed in the following regions 1340–1180 cm^{-1}, for $\nu_{as}OPO^-$, 1180–1080 cm^{-1} for ν_sOPO^-, 1060–940 cm^{-1} for $\nu_{as}POP$ (27), and 850–680 cm^{-1} for ν_sPOP. Frequencies below 670 cm^{-1} are attributed to the bending, the translation, and the rotation of the P_6O_{18} ring; C–C bending and NH_3 torsion may occur in this region. Those frequencies over 1340 cm^{-1} correspond to N(O, C)–H stretching and bending modes (28).

The stretching modes of P_6O_{18} ring and band assignments are described in Table 7. Observed doublet IR frequencies (1260–1240 cm^{-1}), (1130–1120 cm^{-1}), (960–940 cm^{-1}), and (790–780 cm^{-1}) in each stretching domain are assigned to A_u modes issuing from the activation and the splitting of E_{2u} in the $\nu_{as}OPO^-$ domain and the splitting of E_{1u} in the ν_sOPO^-, ν_sPOP, ν_sPOP domains, respectively.

TABLE 7

IR Frequencies (cm^{-1}) and Assignments in the Stretching Domain of P_6O_{18} Ring in $[NH_3–(CH_2)_2–NH_2–(CH_2)_2–NH_3]_2P_6O_{18} \cdot 2H_2O$

	$P_6O_{18}:D_{6h}$			$P_6O_{18}:C_i$			
Motions	IR	Ra	Modes	Modes	Ra	IR	Obs. IR frequencies (cm^{-1})
$\nu_{as}OPO^-$	+	−	A_{2u}	A_u	−	+	1280 sh
	−	−	B_{2g}	A_g	+	−	
	−	+	E_{1g}	A_g	+	−	
				A_g	+	−	
	−	−	E_{2u}	A_u	−	+	1260 vs
				A_u	−	+	1240 vs
ν_sOPO^-	−	−	B_{1u}	A_u	−	+	1150 w
	−	+	A_{1g}	A_g	+	−	
	−	+	E_{2g}	A_g	+	−	
				A_g	+	−	
	+	−	E_{1u}	A_u	−	+	1130 s
				A_u	−	+	1120 s
$\nu_{as}POP$ + ν(C–C)	−	+	E_{2g}	A_g	+	−	1060 s
				A_g	+	−	1040 s
	−	−	B_{2u}	A_u	−	+	1020 s
	−	−	A_{2g}	A_g	+	−	
	+	−	E_{1u}	A_u	−	+	960 vs
				A_u	−	+	940 vs
ν_sPOP + ν(C–C)	−	+	E_{2g}	A_g	+	−	
				A_g	+	−	
	+	−	E_{1u}	A_u	−	+	790 sh
				A_u	−	+	780 s
	−	−	B_{1u}	A_u	−	+	720 w
	−	+	A_{1g}	A_g	+	−	670 w

Note. vs, very strong; s, strong; w, weak; sh, shoulder.

TABLE 8

Summary of Observed IR Frequencies of Cation Chain and Water Molecule out of the Stretching Domain of the P_6O_{18} Ring in $[NH_3–(CH_2)_2–NH_2–(CH_2)_2–NH_3]_2P_6O_{18} \cdot 2H_2O$

$\bar{\nu}$ (cm^{-1})	Attributions	$\bar{\nu}$ (cm^{-1})	Attributions
3460 m 3340 m 3020 s 2920 s 2880 s 2840 s	$\nu(OH_2)$ + $\nu(NH_3)$ + $\nu(NH_2)$ + $\nu(CH_2)$	1480 w 1460 vw 1450 vw 1440 vw 1410 vw 1400 vw 1380 vw	$\delta(CH_2)$ + $\rho(CH_2)$ + $\omega(CH_2)$
2740 s		1340 sh	
2680 sh		1320 sh	
2600 m			
2580 sh 2540 m 2460 sh 2360 sh 2300 vw 2200 vw 2140 vw 2120 vw	Bands of combination and harmonics	600 w 550 sh 540 s 520 s 480 s 450 m 400 vw 380 vw 360 vw 290 w	$\delta(OPO^-)$ + $\delta(POP)$ + NH_3 rocking + C–C bending + NH_3 torsion
1670 sh 1660 w 1630 m 1600 w 1570 m 1515 vw	$\delta(OH_2)$ + $\delta(NH_3)$ + $\delta(NH_2)$		

Note. s, strong; m, middle; w, weak; vw, very weak; sh, shoulder.

Single frequencies, 1280 cm^{-1} ($\nu_{as}OPO^-$), 1150 cm^{-1} (ν_sOPO^-), 1020 cm^{-1} (ν_sPOP), and 720 cm^{-1} (ν_sPOP) assigned to A_u mode with C_i symmetry arise from the active A_{2u} and from the activation of B_{1u} and B_{2u} modes of D_{6h} ideal symmetry. It is noted that the supplementary frequencies in the ν_{as}POP and ν_sPOP domains are attributed to the stretching ν(C–C). The results for IR-active internal modes of cation chains and water molecules in the title compound are summarized in Table 8. Nevertheless, it must be noted that the assignment of the absorption bands in these regions is only of a tentative character due to the lack of P_6O_{18} IR data and the structure of the complex, which can induce some coupling between organic chains and cyclic anions as a result of the small volume [667.9(6) Å^3] of the cell and the long chain of the organic cation.

V. CONCLUSION

A new cyclohexaphosphate with the protonated nitrogen atoms of aza-3 pentanediyl-1,5 diamine has been synthesized and investigated by thermal analysis, X-ray diffractometry, and vibrational spectroscopy. The DSC heating curve, for the nonmelted anhydrous powder specimen obtained by heating the title compound in a carbolite furnace, shows one endothermic effect preceded by a glass transition. The anhydrous compound melts and it does not crystallize when cooled at room temperature but instead becomes a supercooled liquid. Bond distances and angles in the P_6O_{18} ring anion are examined and, when compared to those observed in the P_3O_9 and P_4O_{12} rings, only the P–P–P angles present very large deviations from the ideal value (120°). All external oxygen atoms are involved in hydrogen bonding. The organic trication is linked to four P_6O_{18} rings to form an anion complex. A three-dimensional network of water molecule hydrogen bonds interconnects the complex anions. These are equal numbers of potential hydrogen bond donors and acceptors in this structure: eight N–H and two O–H donors, and ten O or OH acceptors.

ACKNOWLEDGMENTS

A. J. sincerely thanks Professor K. Sbaï (Faculté des Sciences Ben M'sik, Université Casa.II, Morocco), for his helpful discussions about the IR part of this work.

REFERENCES

1. U. Schülke and R. Kayser, *Z. Anorg. Allg. Chem.* **531,** 167 (1985).
2. E. J. Griffith and R. L. Buxton, *Inorg. Chem.* **4,** 549 (1965).
3. A. Durif and M. T. Averbuch-Pouchot *Acta Crystallogr. Sect. C* **45,** 1884 (1989).
4. A. Durif and M. T. Averbuch-Pouchot *Acta Crystallogr. Sect. C* **46,** 2026 (1990).
5. M. T. Averbuch-Pouchot and A. Durif *Acta Crystallogr. Sect. C* **47,** 1579 (1991).
6. M. T. Averbuch-Pouchot and A. Durif, *Eur. J. Solid State Inorg. Chem.* **28,** 9 (1991).
7. A. Boulle, *C. R. Seances Acad. Sci.* **206,** 517 (1938).
8. S. Kamoun, A. Jouini and A. Daoud, *Acta Crystallogr. Sect. C* **46,** 1481 (1991).
9. M. Bdiri and A. Jouini, *Eur. J. Solid State Inorg. Chem.*, **26,** 585 (1989).
10. A. Jouini and A. Durif, *C. R. Acad. Sci.* **297,** 573 (1983).
11. Enraf–Nonius, "Structure Determination Package." Version RSX11M. Enraf-Nonius, Delft, The Netherlands, 1979.
12. P. Main, S. E. Hull, L. Lessinger, G. Germain, J. P. Declercq, and M. M. Woolfson, "MULTAN77, A System of Computer Programs for the Automatic Solution of Crystal Structures from X-ray Diffraction Data." University of York, England, and Catholic University of Louvain, Belgium 1977.
13. T. Ozawa, *J. Therm. Anal.* **2,** 301 (1970).
14. H. E. Kissenger, *Anal. Chem.* **29,** 1702 (1957).
15. N. N. Chudinova, L. A. Borodina, U. Schülke and K. H. Jost, *Izv. Akad. Nauk, SSSR, Neorg. Mat.* **25,** 459 (1989).
16. M. Rzaigui, *J. Solid State Chem.* **89,** 340 (1990).
17. W. Baur, *Acta Crystallogr. Sect. B* **30,** 1195 (1974).
18. A. M. Prima, *Opt. Spectrosc.* **9,** 236 (1960) [*Opt. Spektrosk.* **9,** 452 (1960)].
19. F. Matossi, *J. Chem. Phys.* **17**(8), 679 (1949).
20. D. E. C. Corbridge and E. J. Love, *J. Chem. Soc.* 493 (1954).
21. P. Tarte, A. Rulmont, K. Sbai, and M. H. Simonot-Grange, *Spetrochim. Acta A* **43**(3), 337 (1987).
22. A. Jouini and M. Dabbabi, *J. Soc. Chim. Tunisie* **2** (6), 29 (1987).

23. A. Jouini, M. Soua, and M. Dabbabi, *J. Solid State Chem.* **69,** 135 (1987).
24. G. Foumakoye, R. Rulmont, and P. Tarte, *Spectrochim. Acta Part A* **46**(8), 1245 (1990).
25. A. N. Lazarev, *Opt. Spectrosc.*, **12,** 28 (1968), [*Opt. Spektrosk.* **12,** 60 (1968)].
26. A. N. Lazarev, "Vibrational Spectra and the Structure of Silicates." Science Press, Leningrad, Russia, 1968.
27. A. Rulmont, R. Cahay, M. Liegeois-Duyckaerts, and P. Tarte, *Eur. J. Solid State Inorg. Chem.* **28,** 207 (1991).
28. Z. Iqbal, H. Arend and P. Wachter, *J. Phys. C: Solid State Phys.* **14,** 1497 (1981).